CHARACTERIZATION OF CHANGES INDUCED BY LINEAGE COMMITMENT AND EXTERNAL MECHANICAL STIMULI ON CELLULAR ULTRASTRUCTURE OF ADULT MESENCHYMAL STEM CELLS

A Thesis Submitted to
the Graduate School of Engineering and Science of
İzmir Institute of Technology
in Partial Fulfillment of the Requirements for the Degree of

MASTER OF SCIENCE

in Biotechnology

by
Levent DEMİRAY

July 2014
İZMİR

We approve the thesis of **Levent DEMİRAY**.

Examining Committee Members:

_____

Assist. Prof. Dr. Engin ÖZÇİVİCİ
Department of Mechanical Engineering
İzmir Institute of Technology

_____

Assist. Prof. Dr. Onursal ÖNEN
Department of Mechanical Engineering
İzmir Institute of Technology

_____

Prof. Dr. Volga BULMUŞ
Department of Chemical Engineering
İzmir Institute of Technology

25 June 2014

_____

Assist. Prof. Dr. Engin ÖZÇİVİCİ
Supervisor, Department of Mechanical Engineering
İzmir Institute of Technology

_____

Prof. Dr. Volga BULMUŞ
Head of the Deoartment of Biotechnology
And Bioengineering

_____

Prof. Dr. R. Tuğrul SENGER
Dean of the Graduate School of
Engineering and Sciences

ACKNOWLEDGMENTS

This thesis is dedicated to my family Mesure DEMİRAY, Deniz DEMİRAY, Mehmet DEMİRAY and Hikmet DEMİRAY who have always believed me. I would like to thank to my family for their constant encouragement and support.

I would like to thank to my advisors, Dr. Engin ÖZÇİVİCİ and Dr. Gülistan MEŞE ÖZÇİVİCİ, for their understanding, kindness, patience and constant support throughout my graduate education. Their continuous guidance is greatly appreciated. I am also grateful to the other committee members for the guidance.

I would like to appreciate deeply my colleagues Veysel BAY, Öznur BASKAN, Melis OLÇUM, Hande AYPEK, Talip ZENGİN and Yusufcan UZ.

Finally, I would like to express my special thanks to my friends Seçkin, Ozan, Ömer, Emrah, Mert, Erdem, Mehmet, Zehra, Çisem, Gizem, Hamza, Sırma, Aysel and others for their encouragement, support and patience during this graduate work.

ABSTRACT

CHARACTERIZATION OF CHANGES INDUCED BY LINEAGE COMMITMENT AND EXTERNAL MECHANICAL STIMULI ON CELLULAR ULTRASTRUCTURE OF ADULT MESENCHYMAL STEM CELLS

Mechanical vibrations have great impact on the regulation of bone cells and their precursor's Mesenchymal stem cells. Anabolic effects of high frequency low magnitude mechanical vibrations on these cells are well identified whereas sensing mechanism of cells and their early response to mechanical stimuli is largely unknown. Here, we hypothesed that daily bouts of low intensity vibrations will affect cellular ultrastructure and the effect will interact with the osteogenic induction. To test this hypothesis mouse bone marrow stem cell line D1 ORL UVA were subjected to mechanical vibrations (0.15g, 90 Hz, 15min/d) for 7 days to both during quiescence and osteogenic commitment. Ultrastructural changes were identified on cellular and molecular levels.

To characterize alterations in cell surface, Atomic force microscopy is used. Mechanical vibrations increased cell surface height, cell surface roughness and nucleus height significantly during quiescence and under osteogenic conditions. Moreover, in order to identify the changes in cytoskeleton structure, actin were stained with phalloidin and imaged with inverted microscope. To quantify phalloidin signals pixel frequency analysis were performed, signal intensities and thickness of actin fibers were measured. It was observed that mechanical stimulation and osteogenic induction effects number of actin fibers and their thickness significantly. Molecular level analysis of cytoskeleton elements and osteogenic markers were performed with Real time RT-PCR. Significant increases in osteogenic markers were detected with osteogenic induction. Unlikely, no relation between mechanical stimulation and osteogenic marker expression was observed.

These results indicate that mesenchymal stem cells responds to mechanical vibrations by altering their ultrastructure in particular cytoskeleton during both quiescence and osteoblastogenesis.

ÖZET

ERİŞKİN KÖK HÜCRELERİNDE DOKU YÖNELİMİ VE DIŞ MEKANİK ETKİLERE BAĞLI GELİŞEN ALT YAPISAL DEĞİŞİKLİKLERİN KARAKTERİZASYONU

Kemik hücrelerinin ve kemik oluşumunu sağlayan erişkin kök hücrelerinin regülasyonunda mekanik kuvvetlerin etkisi büyüktür. Yüksek frekanslı, düşük yoğunluklu meknik titreşimlerin bu hücre tipleri üzerindeki yapıcı etkileri araştırmalarla ortaya konmuş fakat hücrelerin bu titreşimleri algılama yolakları çözülememiştir. Bu çalışmada düşük yoğunluklu, yüksek frekanslı mekanik titreşimlerin, erişkin kök hücrelerine düzenli olarak uygulanmasının, hücre altyapısında değişikliklere neden olacağı hipotez edilmiştir. Bunu test etmek için fare erişkin kök hücreleri, 7 gün boyunca, günde 15 dk mekanik titreşimlere mağruz bırakılmış, bağzı deney grupları eş zamanlı olarak doku yönelimine sokulmuş ve hücre alt yapılarında ki değişim hücresel ve moleküler düzeyde gözlemlenmiştir.

Hücre yüzeyinde meydana gelen değişimleri karakterize etmek için Atomik Kuvvet Mikroskobu kullanılmış ve hücre yüzeyinin yüksekliği ve pürüzlülüğünde önemli artışlar gözlenmiştir. Ayrıca hücre iskeletindeki değişimleri gözlemlemek için Aktin proteini phalloidin boyasıyla boyanmış ve Florasan mikroskobuyla incelenmiştir. Yapılan analizler sonucunda mekanik titreşimlerin hücre iskeletindeki aktin protein miktarını ve aktin iplikçik kalınlığını arttırdığı gözlemlenmiştir. Son olarak hücre iskeletini oluşturan ve doku yöneliminde rol oynayan diğer birtakım proteinlerin gen ifade analizleri Real Time RT-PCR ile yapılmıştır.

Bulunan sonuçlar erişkin kök hücrelerin, doku yöneliminden bağımsız olarak, düşük yoğunluklu, yüksek frekanslı mekanik titreşimlere hücre altyapılarını yeniden düzenleyerek tepki verdiklerini göstermiştir.

TABLE OF CONTENTS

LIST OF FIGURES

Figure **Pages**

LIST OF TABLES

Table **Pages**

CHAPTER 1

INTRODUCTION

1.1. Mesenchymal Stem Cells

There are two distinct stem cell types residing in bone marrow: Hematopoietic stem cells (HSCs) and Bone marrow stromal cells. At birth long bones are full of red bone marrow containing HSCs. In the fifth to seventh year, adipose stem cells begin to replace red bone marrow in long bones and forms yellow bone marrow which contains bone marrow stromal cells. In adults, red bone marrow is located in axial and proximal parts of long bones and yellow bone marrow is in the middle site (Krause, 2007). HSCs are responsible for maintenance of hematopoietic system by differentiating into blood cells (Short et al., 2004). Bone marrow stromal cells or Mesenchymal stem cells (MSCs) are stromal cells that have capacity to self-renewal and differentiate in to mesenchymal tissues such as bone, adipose, cartilage or muscle (Ding et al., 2011) (Figure 1.1). The term stroma signifies the supporting connective tissue associated with the dominant functional tissue in an organ. In bone marrow the term stroma describes the non-hematopoietic connective tissue parts that provide a system of structural support for developing hematopoietic cells as well as the functional support for the hematopoiesis process by creating unique microenvironment that provides appropriate regulatory growth molecules, cell-cell and cell-extracellular matrix interactions (Short et al., 2004). The main functions of MSCs is to provide replacement and repair descendants for normal turnover or injured tissues(Caplan, 2005).

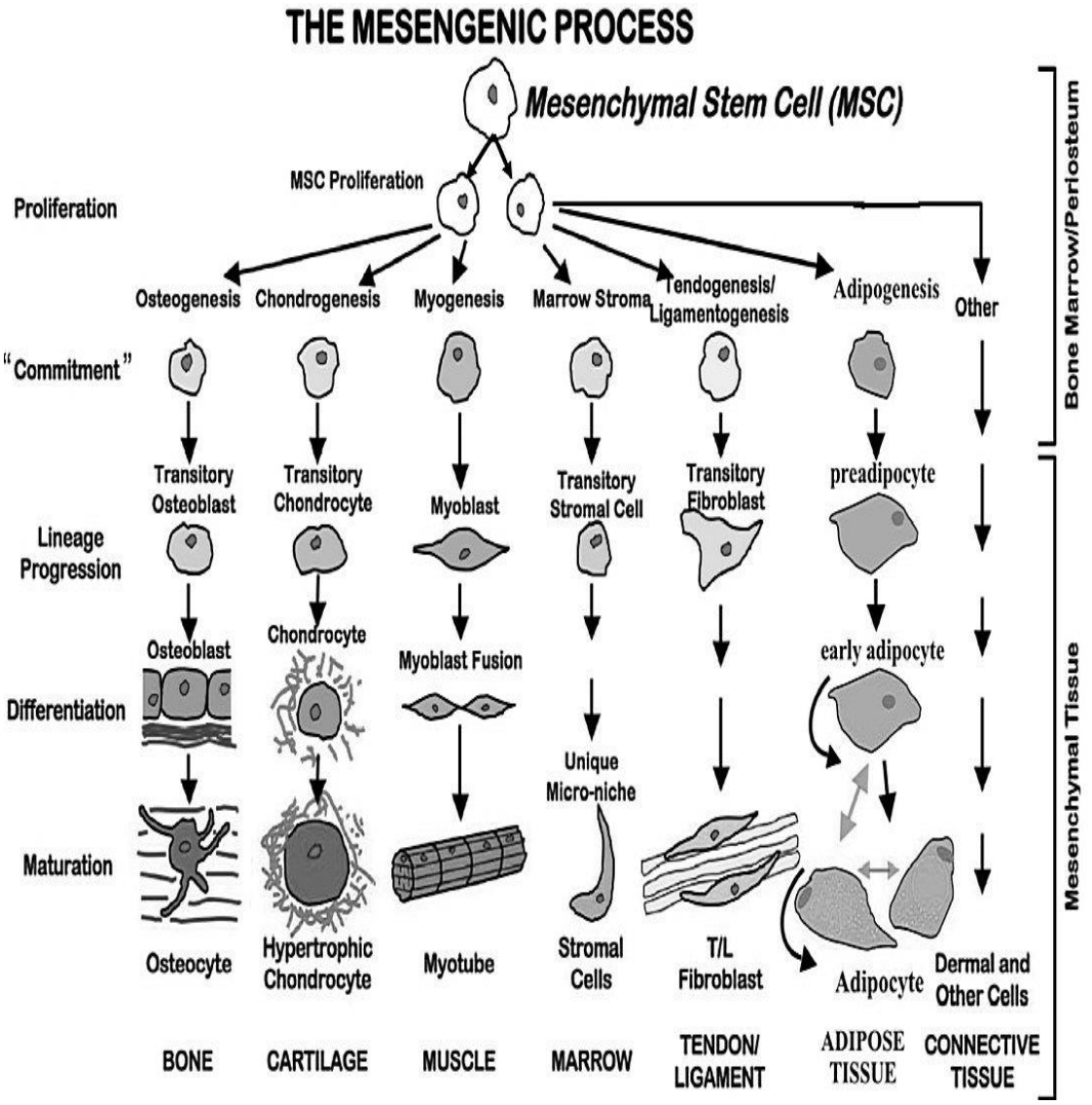

Figure 1.1. Illustration of the mesengenic process. Mesenchymal stem cells (MSCs) are present in yellow bone marrow, and connective tissues such as adipose, muscle, cartilage. These cells function as replacement units for differentiated cell types that expired or succumbed to injury or disease. MSCs are able to differentiate into distinct mesenchymal tissue types such as bone, adipose and muscle tissue. This differentiation event is regulated by growth factors, hormones and cytokines, and multistep lineages are involved in it (Source: Caplan, 2005).

1.2. Bone Tissue

Skeleton is formed by bone tissue and there are two distinct type of bone : cortical (compact) and trabecular (cancellous). Cortical bone is more dense tissue comparing with trabecular bone. Compact bone is mainly found in shaft of long bones

and blood vessels penetrate into it via canaliculi. Trabecular bone has porous structure and is found at the end of long bones, near joint surfaces and in vertebrae (Ruimerman, 2005). The skeleton is a metabolically active organ that under goes continuous remodeling throughout life. In the body, bones serve five main functions. First it provides structural support and robustness to the body as a framework. It also assists to movement of body by working with skeletal muscles, tendons, joints and ligaments. Muscles responsible for movement are attached to bones and their contraction provides movement via bones. Further, it serves as reservoir for calcium and phosphate needed for the maintenance of serum homeostasis by contributing to buffering changes in hydrogen ion concentration. Moreover, it is responsible for production of blood cells. This event occurs at red bone marrows located in long bones. Finally, it protects bone marrow and vital internal organs such as brain, lungs and heart (Sommerfeldt and Rubin, 2001) (Rodan, 2003). Bone tissue undergoes continuous remodeling that is the process by which bone is being turned over, allowing the maintenance of the shape, quality and size of the skeleton. This is accomplished by repairing of microcracks and modification of structure in response to stress and other biomechanical forces (Hadjidakis and Androulakis, 2006).

Bone modeling and remodeling are defined as different phenomena. Bone modeling event occurs in response to altered mechanical loads and is brought about by continuous bone resorption and formation. Modeling process can happens at different parts of bone and can alter bone morphology (Frost, 1990a). Under normal conditions, in order to maintain bone quality and integrity, old bone tissue is replaced with new tissue. In this case, resorbtion and formation rates are equal and this causes no morphological change in bone. This is called remodeling (Frost, 1990b). The remodeling and modeling processes begins with recruitment of osteoclasts at renewal site Osteoclast cells are large multinucleated cells that form by fusion of mononucleated precursor cells with hematopoietic origin(Salo et al., 1996) (Figure 1.2 A). They attach to the bone tissue matrix and form a ruffled border at the bone/osteoclast interface. Following that, the osteoclast acidifies the micro environment and dissolves the organic and inorganic matrices of the bone. Just after the formation of resorptive pits, osteoblast cells are recruited to the resorption site. The osteoblasts are derived from MSCs in bone marrow (Figure 1.2B). These cells simply deposit osteoid and mineralize it to form new bone tissue. As forming new bone, some of osteoblasts are encapsulated in the osteoid matrix and differentiate to osteocytes. Remaining osteoblasts continue to synthesize

bone until they eventually stop and transform to quiescent lining cells that completely cover the newly formed bone surface. These lining cells are highly interconnected with the osteocytes in the bone matrix through a network of canaliculi (Väänänen et al., 2000).

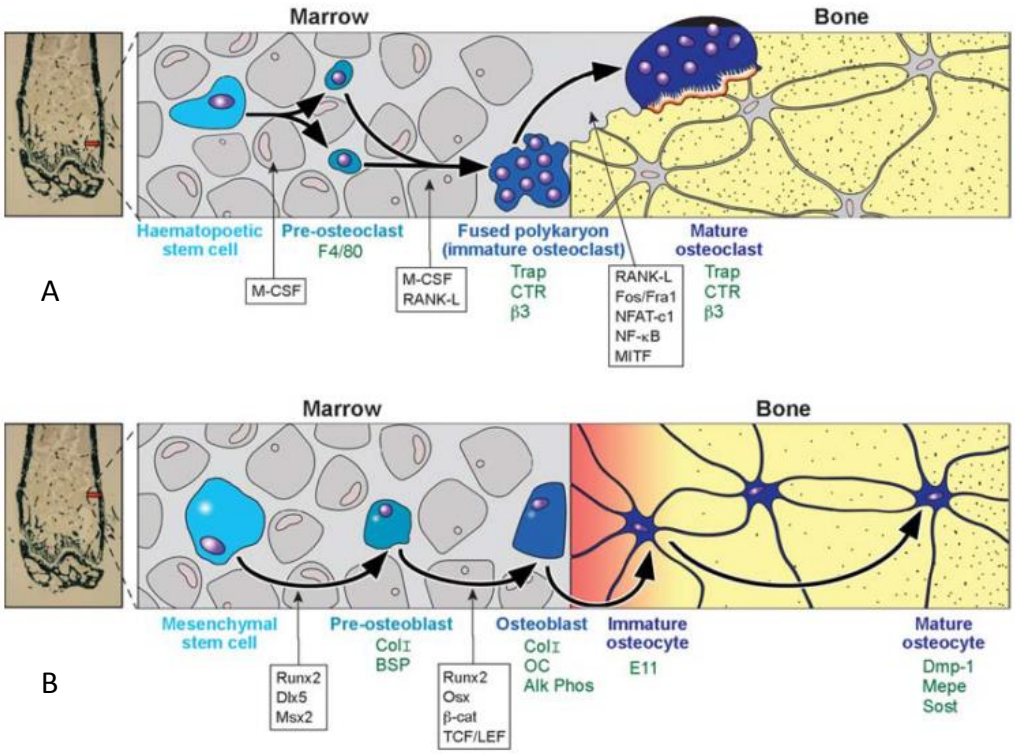

Figure 1.2. Osteoclast and osteoblast lineages. Hematopoeitic stem cells (HSCs) are precursors of blood cells and found in red bone marrow, liver and spleen. Osteoclast cells are differentiated from HSCs in red bone marrow. Macrophage stimulating factor (M-CSF) is needed for proliferation of mononuclear cells from precursor HSCs. These preosteoclasts expressing F4/80 surface antigen enter to the blood circulation and find the resorbtion site on bone. Then they start to fuse together and form polykaryon immature osteoclast in the presence of M-CSF and RANK-L. After that these polykaryons turn into mature osteoclasts and do their functions. (A). Osteoblast cells have mesenchymal origin. By expression of Runx2, Dlx5 and Msx2 precursors star to for preosteoblasts. Further expression of Runx2, osterix and Wnt signaling proteins (β-catenin, TCF/LEF1) plays role in mature osteoblast formation. Now mature osteoblasts are able to form osteocytes by expressing early osteocyte marker E11, dentin matrix acidic phosphoprotein 1 (DMP-1), Sclerostin (Sost) and Matrix extracellular phosphoglycoprotein (Mepe) (B) (Source: Robling et al., 2006).

1.3. Regulation of Bone Remodeling

Bone tissue in most mammals consists of four main envelopes: the periosteal, endocortical, trabecular and intracortical. These envelopes differs in surface area volume ratio and their response to different stimuli (Robling et al., 2006). Bone remodeling takes place in each of these envelopes and remodeling process is controlled both systemically and mechanically

1.3.1. Systemic Regulation

There are four main hormone regulating bone remodeling procedure. Parathyroid (PTH), calcitonin and vitamin D3 maintain critical serum calcium level within precise physiological limits (2.2-2.6 mM) by controlling osteoclastic bone resorption. Calcitonin receptors are expressed by osteoclasts and play role in inhibition of osteoclastic resorption (Zaidi et al., 2002). Unlikely, PTH binds to its receptors on osteoblasts and MSCs and indirectly stimulates osteoclastic bone resoption by activating expression of MCSF and RANKL through signaling by cAMP responsive element binding protein (CREB). Another non skeletal task of PTH is to control increased renal reabsorbtion of calcium which maintains physiological serum calcium level together with elevated resorption to mobilise calcium from bone. Vitamin D3 inactive precursor is also activated by PTH (Roy V. Talmage, 1958). Activated vitamin D3 stimulates calcium absorption from the gut and the kidney. Estrogen is another regulator of bone remodeling event. It is a bone sparing hormone acting on both osteoblasts and osteoclasts. Osteoclast life span is controlled by this sex hormone by triggering apoptosis through Fas and Fas ligand signaling. Therefore decreased level of oestrogen causes elevated osteoclast survival and function in women after menopause. It also plays a role in response of bone to mechanical stimulation (Zaman et al., 2006) (Krum et al., 2008).

1.3.2. Mechanical Regulation

Bone remodeling is also regulated by external mechanical forces (Chen et al., 2010) (Jacobs et al., 2010). Bone metabolism is affected locally or systematically by forces. For instance, serving arm of tennis player has more condensed and strong bone compering with other arm (locally) or profound bone loss is observed in astronauts experiencing zero gravity (systemically). It has shown that individual bone cells osteoblasts, osteoclasts and osteocytes respond to mechanical signal. Also whole animal experiments confirmed that there is a response in tissue level as well. Wnt signaling proteins, prostaglandins and nitric oxide are some of the early signaling molecules produced by bone cells (Bonewald and Johnson, 2008). In osteocytes, β- catenin level rapidly increases in nucleus region just after mechanical stimulation suggesting activation of Wnt signaling or cadherin mediated signaling. Even though microcracks in bone tissue are thought to be crucial driver of the remodeling event, the exact mechanism underlying mechanosensation remains unclear (Norvell et al., 2004) (Santos et al., 2010). Despite this, the profound anabolic effects of mechanical forces on bone have prompted the development of mechanical therapies to prevent bone loss and increase bone mass.

1.4. Mechanical Forces and Bone

Mechanical forces, pressure, temperature, gravity, magnetic field etc.., have been acting on organisms since the beginning of life on earth. All living things have adapted to changes in their physical environment and passed their adapted genetic material to the next generation successfully. In time, some tissues and organs have become unable to function properly in the absence of some of these forces.

Bone is metabolically active organ and function of this organ is strictly dependent of mechanical forces such as gravity, blood pressure and muscle strains. In the last 10 years, anabolic effects of mechanical forces on bone have been described extensively (Rubin et al., 2001) (Rubin et al., 2004) (Ozcivici et al., 2007) (Verschueren et al., 2004) (Judex et al., 2007) (Yen K Luu et al., 2009) (Sehmisch et al., 2009) (Ozcivici et al., 2010) (Chen et al., 2010) (Arnsdorf et al., 2010) (Lau et al., 2010).

These effects can be simply observed in real life. For instance, professional sport players have more dense and strong bones in their dominant arms and legs (Jones et al., 2007) (Heinonen et al., 1995). In contrary, disuse of limbs, long term bed rest and zero gravity environment makes bone weaker by decreasing its density (Meloni et al., 2011) (Lang et al., 2004). It should be also noted that mechanical forces are not only determinants of bone quality. Genetic factors, sex, age, ethnicity and diet are critical parameters for bone health (Judex et al., 2004) (Peacock et al., 2005) Mechanical forces can also be delivered as low magnitude high frequency (LMHF) vibrations and this mode of loading has been utilized as mechanical stimuli for cell culture, animal and human experiments (Judex et al., 2007) (Garman et al., 2007). As an anabolic agent, LMHF vibrations are good candidate for the treatment and prevention of osteoporosis, osteoarthritis and osteopenia due to being noninvasive, drug-free and applicable for everyone (Rubin et al., 2006). According to results of long-term animal studies with osteopenia mouse model, LMHF whole body vibrations increased trabecular bone density. Also increase in bone stiffness, strength and quality was observed (Sehmisch et al., 2009). Moreover, LMHF vibrations can inhibit the resorption of bone in disuse osteoporosis. Bone formation rate per bone volume (BFR/BV) of tail-suspended mouse model was decreased. When mouse is allowed to weight bear 10 min per day, no significant change was observed in BFR/BV ratio of experiment group. However, when they allowed mice weight bear on vibrating plate (0.3 g, 45 Hz), BFR/BV rate in experiment group was normalized (Rubin et al., 2006).

Whole body vibration experiments were also performed with post-menopausal women. 1 year of two 10 minutes daily exposure of LMHF (2 m/s^2, 30 Hz) whole body vibrations showed a significant effect of compliance on efficiency of the intervention on lumbar spine (Rubin et al., 2004). In another study, 25 post-menopausal women were subjected to whole body vibrations (35-40 Hz, 2.28-5.09 g) while performing static and dynamic knee extensor exercise on vibration plate three times in a week for 24 weeks. At the end of study, significant increase in bone mineral density of hips and no vibration related side effects were observed (Verschueren et al., 2004).

1.5. Mechanical Forces and MSCs

Mechanical forces regulates not only bone cells but also bone precursor MSCs. MSCs residing in bone marrow are able to differentiate into both osteoblasts and adipocytes and mechanical forces such as LMHF vibrations prevents adipogenesis while increasing osteogenesis (Yen Kim Luu et al., 2009). Both osteogenic and adipogenic factors are expressed by MSCs and cross-regulate each other to remain MSCs in their undifferentiated state (Rosen, Evan D, MacDougald, 2006). For instance, Peroxisome proliferator activated receptor gama (PPARɣ), a nuclear hormone receptor that found in most cell but predominantly in adipocytes is one of the factor that regulate adipogenic gene expression and mature, lipid filled, adipocyte formation from MSCs (David et al., 2007). In MSCs, activation of PPARɣ induces the proteosomal degredation of β-catenin (Liu et al., 2006). β-catenin is needed for bone development and Sustained β-catenin level in MSCs lead MSCs to osteogenesis by increasing Runx2 expression (Figure 1.3) . When mechanical stimulation is applied to MSCs, PPARɣ is down regulated and increased β-catenin level favor cell to undergo osteogenesis (David et al., 2007) (Case and Rubin, 2010).

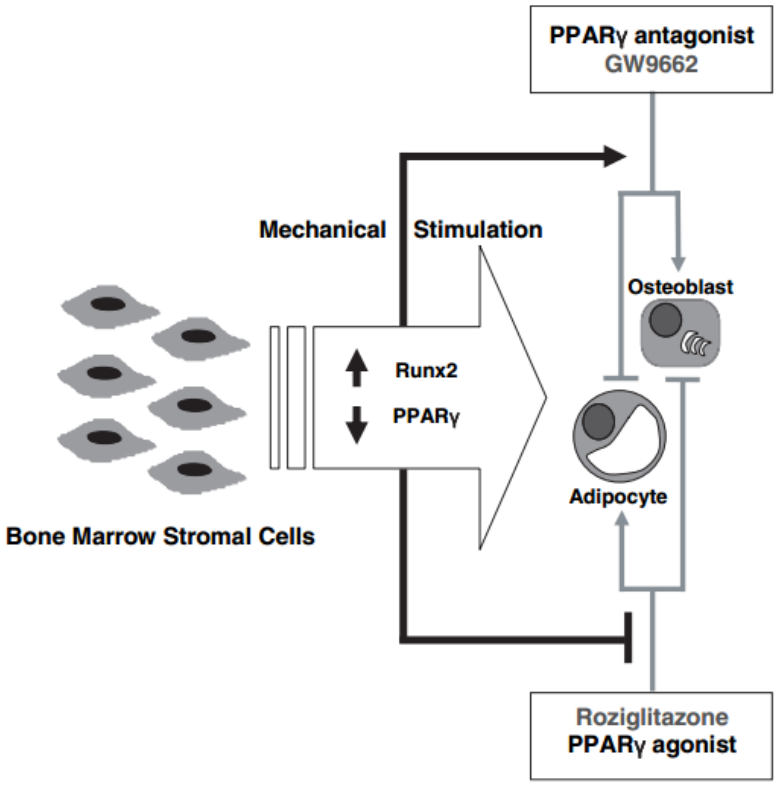

Figure 1.3. The effect of mechanical stimulation on Runx2 expression on MSCs. Osteoblastogenesis is promoted with mechanical stimulation by upregulating Runx2 and downregulating PPAR. A potent PPAR antagonist GW9662 induces the osteogenesis and decrease adipogenesis. Unlikely, rosiglitazone induced PPAR activation promotes adipogenesis by down regulating Runx2. Mechanical stimulation reduced the rosiglitazone activated adipogenesis while increasing osteblastogenesis induced by GW9662 (Source: David et al., 2007)

For all the observed beneficial outcomes related to bone regeneration, the mechanisms for how LMHF vibrations are sensed by cells are largely unknown. However, it is known that small magnitude strains acting on bone during daily activities such as walking or standing are main regulators of bone activity (Fritton et al., 2000).

Fluid shear stresses acting on the cell membrane may be a potential candidate as these loads are shown to be more effective in inducing osteogenesis compared to substrate deformations (Jacobs et al., 2010) (You, 2000). However, recent evidence suggested that fluid flow may not be a good model to simulate low intensity vibrations, as mechanical response may be modulated by global accelerations rather than drag forces acting on the cell membrane during vibratory loading (Uzer et al., 2012).

If accelerations are indeed capable of stimulating mechanotransduction pathways, cellular ultrastructure should be an important determinant of loads translated within the cell, as cytoskeletal network can determine local and global mechanical

properties of cells (Alenghat and Ingber, 2002). Consistent with the observation that adaptations in cellular ultrastructure are required for mechanical transduction, chemical blocking of actin polymerization inhibits the response of bone cells to physical stimuli (Rosenberg, 2003). The adaptive response of cellular ultrastructure to external loads may be required for cytoskeletal elements to effectively direct and regulate loads internally to downstream elements, but it is currently not clear how cellular ultrastructure respond to oscillatory motions, a physical regimen that prescribes loading on cells that may be fundamentally different compared to loads prescribed by fluid flow (Uzer et al., 2013, 2012).

Another important consideration on stem cell ultrastructural adaptations is that during osteogenesis in vitro, marrow stem cells alter their cytoskeletal matrix to become stiffer (Darling et al., 2008) (Yourek et al., 2007). Even though this observation was made in the absence of exogenous mechanical loads, in vivo bone environment never lacks repeated mechanical loads (Fritton et al., 2000) and it is important to determine the interaction between the effect of osteogenesis and mechanical loads on ultrastructural properties. Here we aimed to identify ultrastructural adaptations of bone marrow stem cells to daily low intensity vibrations during early osteogenic commitment. **We tested the hypothesis that daily bouts of low intensity vibrations will affect cellular ultrastructure and the effect will interact with the osteogenic induction.**

CHAPTER 2

MATERIALS AND METHODS

2.1. Cell Culture

Mouse bone marrow stem cell line D1-ORL-UVA (ATTC) was used in all experiments. D1 cells were grown and maintained in Dulbecco's Modified Eagles Medium (D-MEM, Hyclone) with high glucose, L-Glutamine and sodium bicarbonate and supplemented with 10% fetal bovine serum and 1% Penicillin/Streptomycin as suggested by the vendor. For all experiments, D1 cells were used from 6th-12th passages as high passage numbers may be detrimental for the commitment potency of these cells to mesenchymal lineages (Mandana Mohyeddin Bonab 2006). Osteogenic induction is achieved by addition of 1000 μg/ml ascorbic acid (Sigma) and 10 mMol β-glycerol phosphate (Sigma) to the growth medium. For all experiments except atomic force microscopy (AFM), D1 cells were plated at a density of 1×10^4 cells/well in 6-well plates (Corning) on sterilized 22x22 cm^2 glass cover slides and maintained in the growth medium at 37°C and 5% CO2. For AFM experiments cells were grown on sterilized glass slides with a diameter of 1 cm. Cells were allowed to adhere to cover plate for two days and then growth media was either refreshed or changed with osteogenic media. Experiments were terminated at day 9 and culture media was refreshed every 3 days. Four experimental group were used in all experiments.

Table 2.1. Experimental groups used in all experiments

Group	Medium type	Vibration
Growth control (GC)	Growt medium	No
Growth vibration (GV)	Growth medium	Yes
Osteogenic control (OC)	Osteogenic medium	No
Osteogenic vibration (OV)	Osteogenic medium	Yes

MSCs are anchorage dependent cells that can sense, contact and adhere with their microenvironment via extracellular proteins. Therefore, matrix stiffness is an important factor affecting their mechanical properties, proliferation and differentiation (Discher et al., 2009). MSCs on soft substrate are tending to be neurogenic. On stiffer substrates these cells stars to differentiate in time to form harder tissues such as muscle or bone (Tai et al., 2010). Focal adhesions and the cytoskeleton are also influenced by substrate stiffness and change their structure (Bershadsky et al., 2003). Even though 1 week is too short to take substrate stiffness as an important parameter for cell fate, we used glass substrate in all our experiments except the cell growth experiments.

2.2. Mechanical Vibration Application

In an effort to test the effects of low intensity vibrations on adult stem cells with or without osteogenic commitment, cells were either subjected to 90 Hz, 0.15g vibrations for 7 days (15min/day) under room conditions or received sham treatment to eliminate the effects of ambient conditions. Anabolic effects of 90 Hz, 0.15 g mechanical signals were already shown in literature (Sehmisch et al., 2009) (Judex et al., 2007) and we the values chosen accordingly. Proper sinusoidal signals were generated with a function generator (MLP Lab Electronics) that is connected to an amplifier (Spekon Q1000). Amplified electrical signals were translated to mechanical signals through a high capacity speaker (EVP-X) that is connected to a custom made stainless steel platform. Brevity of mechanical signals was measured real time with an accelerometer (Kistler) on platform and monitored with Lab View Signal Express 2010 software 4.0.0. (National Instruments).

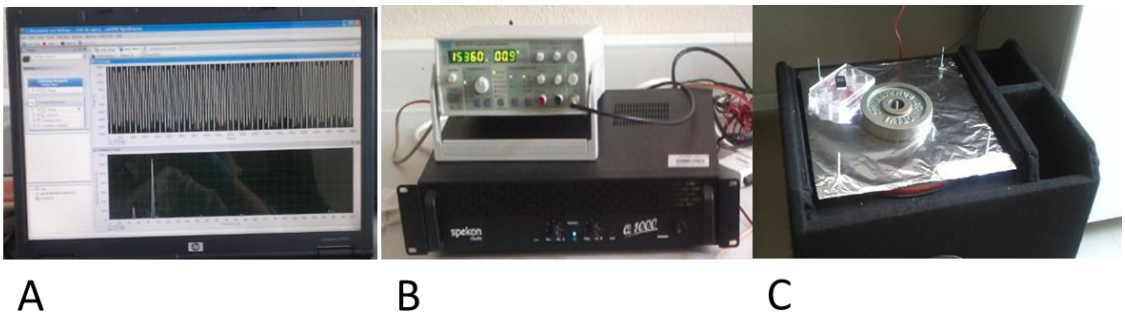

Figure 2.1. Vibration device. Monitoring software Labview Signal Express (A), function generator (Top) and amplifier (Bottom) (B), high capacity speaker (EVP-X) that is connected to a custom made stainless steel platform (C).

2.3. Cell Growth and Viability Assay

At day 9, cover glasses were removed to a new 6 well plate and there cells were trypsinized (2 ml) for 5min at 37C°. Reaction was stopped by the addition of growth medium (2 ml). Total volume was gently pipette for single cell suspension and the volume was transferred a 15 ml conical tube (Corning) and centrifuged for 5 min. Supernatant was discarded and remaining pellet was resuspended in 1 ml growth medium. From this suspension 10µl of volume was transferred to a 1.5 ml tube and there mixed with 90 µl of 0,5 % Trypan blue dye (Invitrogen). Cells from 10 µl of this new suspension were counted with a hemocytometer (Isolab) and number of cells in the original suspension was calculated.

Cell viability was analyzed via MTT assay, in which cells were incubated with 0.5mg/ml MTT (Amresco LLC, USA) for 4 hours. After the incubation tetrazolium salts were dissolved in DMSO and colorimetric measurements were done at 570 nm with a background subtraction at 650 nm.

2.4. Mineralization Assay

Presence of calcified matrix was detected with Alizarin Red assay. Briefly cells were washed (x3) with 1 ml of PBS and fixed with 500 µl of 10% neutral buffered formalin for 30 min. Afterwards, cells were rinsed (x2) with 1 ml of DI water and stained with 1 ml of alizarin red dye (Sigma-Aldrich) for 30 min. Cells were again rinsed (x2) with DI water and then remained in PBS for 15 min to remove non-specific

binding of dye. Micrographs of calcified matrix were obtained through the light field of an inverted microscope (Olympus IX71,).

2.5. Atomic Force Microscopy

Digital Instruments-MMSPM Nanoscope IV (Bruker Multimode) was used to get AFM images. Cells were washed with ultrapure water and dried in ambient conditions for 15 minutes. Cells were probed with a soft silicon cantilever with semi angle of 35° and 8 N/m spring constant. Locations of cells were detected using an optical microscope (Nikon 10x), and cantilever tip was conveniently adjusted above observed cells. In tapping mode, 50x50 μm^2 area was scanned with rate of 1001 Hz and number of sample for each image was 512. Cells were analyzed for average surface height and roughness over cytoplasmic regions and physical characteristics of nucleus using AFM image processing software Gwyddion 2.31.

2.6. Immunostaining and Fluorescent Microscopy

To acquire micrographs of actin structure of MSCs, cells were stained with Phalloidin and DAPI dyes for fluorescent microscopy imaging. Briefly, cells were washed (x2) with 1 ml of 1 % PBS and fixed with 500 µl 4 % paraformaldehyde (PFA) for 20 min. PFA was washed (x3) again with 1% PBS followed by membrane permeabilization with 500 µl of 0.1% TritonX / 1% PBS for 15 min. Agent was blocked with 500 µl of 3% BSA in 0.1% TritonX / 1% PBS for 30 min. Cells were then incubated with phalloidin (Alexa 647, Invitrogen) dye for 30 min in the dark for the imaging of cytoskeletal elements. Cells were washed (x3) with 1% PBS in a dark environment and then incubated in DAPI solution for 10 min for the imaging of cell nucleus. Cells were final washed with DI water and mounted with DABCO (Sigma-Aldrich) mounting medium. Images were acquired with an inverted microscope and fluorescent attachment. Micrographs of actin cytoskeleton were acquired at 573 and nuclear structures were imaged at 460nm A minimum of 10 sample images were used for signal intensity and fiber thickness analysis per condition from three different experiments. All image processing were done using ImageJ 1.47 (NIH) software.

2.7. Gene expression Analysis

Cells were lysed and total mRNA was isolated using purelink RNA mini kit (Invitrogen). After verification of purity and determination of concentration by nanodrop (ND-1000 spectrophotometer), 2 step Real Time PCR was performed. For reverse transcription reaction Revertaid first strand cDNA synthesis kit (Thermo Scientific) was used with 1000 ng template RNA. cDNA samples of 7.5 µl were loaded into 96-well PCR plate (Thermo Scientific) with 12µl of Syber Green (Thermo scientific), 2.5µl forward and reverse primers (Table 1) for quantitative RT-PCR (BioRAD IQ 5 Thermal Cycler). GAPDH is used as housekeeping gene and expression levels of all other proteins are normalized to GAPDH expression level.

Table 2.2. Target genes for Real time RT-PCR, their functions and primers. Primers designed for the gene expression analysis of osteogenic markers (Runx2, OCN) and cytoskeletal elements (β-Actin, Desmin, Vimentin, β-Tubulin, PTK2) for D1 ORL UVA mouse mesenchymal stem cells. GAPDH was used as the house-keeping molecule for all groups.

Target gene	Function	Forward primer	Reverse primer
ALP	Hard tissue formation	TTTAGTACTGGCCATCGGCA	ATTGCCCTGAGTGGTGTTGCA
Runx2	Transcription factor	TCCCTGAACTCTGCACCAAGT	TTCCGTCAGCGTCAACACCAT
OCN	Bone formation	CTGAACAAAGCCTTCATGTCCAA	GCGCCGGAGTCTGTTCACTA
Collagen1a1	Bone formation	CACCCTCAAGAGCCTGAGTC	AGACGGCTGAGTAGGGAACA
Desmin	Intermediate filament	GTGAAGATGGCCTTGGATGT	GTAGCCTCGCTGACAACCTC
Vimentin	Intermediate filament	ACGGTTGAGACCAGAGATGG	CGTCTTTTGGGGTGTCAGTT
β-Actin	Actin filament	CTTCTTTGCAGCTCCTTCGTT	TTCTGACCCATTCCCACCA
PTK2	Cellular adhesion	TTGGACCTGGCATCTTTGAT	AGAACATTCCGAGCAGCAAT
GAPDH	House keeping	GAC ATG CCG CCT GGA GAA AC	AGC CCA GGA TGC CCT TTA GT

2.8. Statistical Analysis

Statistical analysis of all results was performed with unpaired t-test within 95% confidence interval, control and experiment groups in growth and osteogenic medium were compared with each other. Microscopy (both fluorescence and atomic force) samples were maintained and measured together in the same days for growth and osteogenic groups, therefore comparisons were only made within groups. Samples that were used for gene expression analysis were maintained and measured together for all.

CHAPTER 3

RESULTS AND DISCUSSIONS

3.1. Cell Growth and Viability Assay

In order to identify effects of LMHF vibrations on MSCs proliferation, cell count with hemocytometer was performed after 7-days mechanical stimulation. Proliferation of MSCs in quiescence was elevated by LMHF vibrations by 7% ($p=0.04$) (figure 3.1 A). Proliferation of MSCs under osteogenic conditions was also increased by mechanical stimulation by 66% ($p<0.01$) (figure 3.1.B)

MTT assay showed that mechanical vibration increased cell viability by 1% ($P = 0.05$). Similarly, OV cells 3% more viable than OC cells ($P < 0.01$). There is not much difference between groups but results are statistically significant.

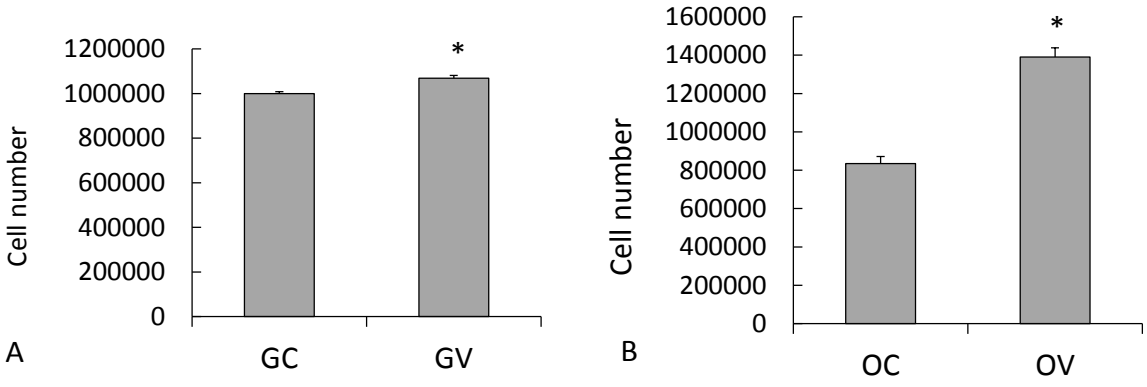

Figure 3.1. Results of cell count with hemocytometer. In both groups, mechanical stimulation elevated cell proliferation significantly.(*: $p<0.05$)

Table 3.1. Cell viability by MTT assay. Results are presented mean ± SD, *: P < 0.05 between growth control and vibration groups. †: P < 0.05 between growth control and vibration groups.

Group	Number of cells [x 10^5 /ml]	Cell Viability [a.u.]
GC	0.98 ± 0.17	3.46 ± 0.05
GV	1.10 ± 0.25 *	3.51 ± 0.07 *
OC	1.54 ± 0.61	3.40 ± 0.06
OV	1.72 ± 0.36	3.49 ± 0.06 †

3.2. Mineralization Assay

Mineralization assay with alizarin red dye prove that MSCs undergo osteogenesis with osteogenic induction. Red parts in the figure 3.2 shows calcified matrix in MSCs under osteogenic differentiation.

A 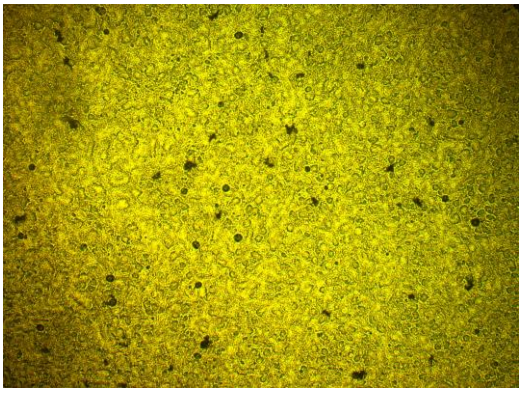 B 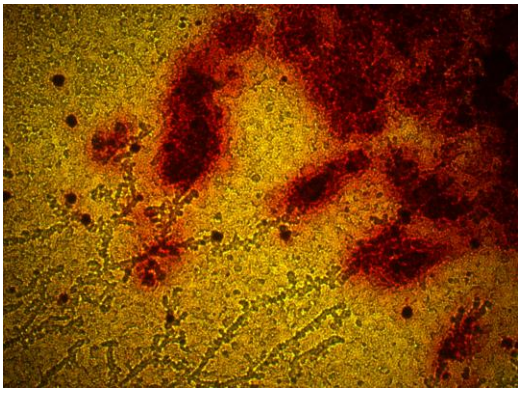

Figure 3.2. Alizarin red staining. The cells in quiescence have no calcium deposits (A). The cells under osteogenic conditions deposit calcium and alizarin red dye stain that calcified matrix (B).

3.3. Atomic Force Microscopy

Mechanical vibrations effected morphology of cells significantly. Average nucleus height of GV and OV cells increased by 70% ($p<0.01$) and 20% ($p=0.052$) (figure 3.3 A).

Average cell surface height of vibrated MSCs was 87.14% ($p<0.01$) higher than control group. MSCs under osteogenic conditions showed no significant change in average cell surface height. Additionally osteogenic induction increased average cell surface height of MSCs by 78.18% ($p<0.01$) (figure 3.4 A). Average cell surface

roughness difference between vibration and control groups of MSCs was not statistically significant, whereas under osteogenic conditions vibrated cells have 22% higher (p=0.013) average cell surface roughness than control group (figure 3.4 B).

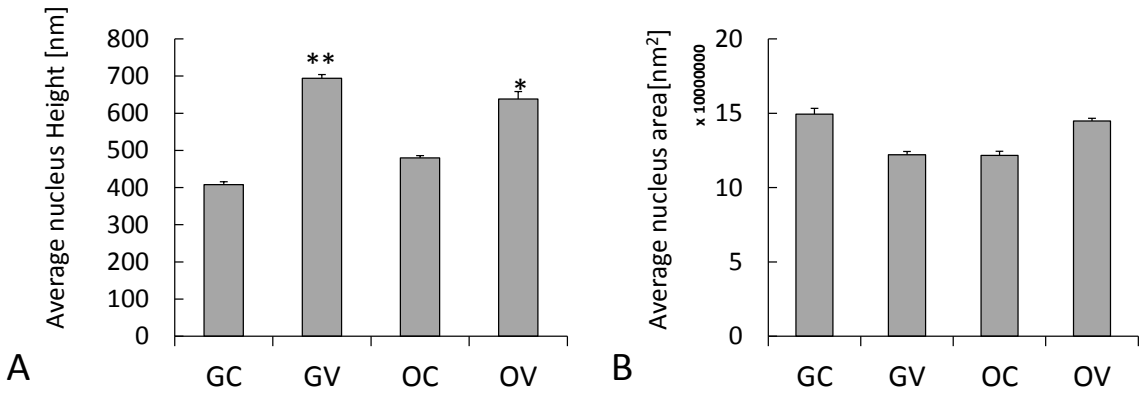

Figure 3.3. In growth medium (GV-GC), LMHF vibrations increased the average nucleus height of MSCs 70%. Under osteogenic conditions (OC-OV), nucleus height of cells was increased with LMHF vibrations by 33% (A). No significant change in average nucleus area was observed in between groups (B). For GC: n=16, GV:n=14, OC: n=25, OV: n=10 sample were analized. (*: $p<0.05$, **: $p<0.01$)

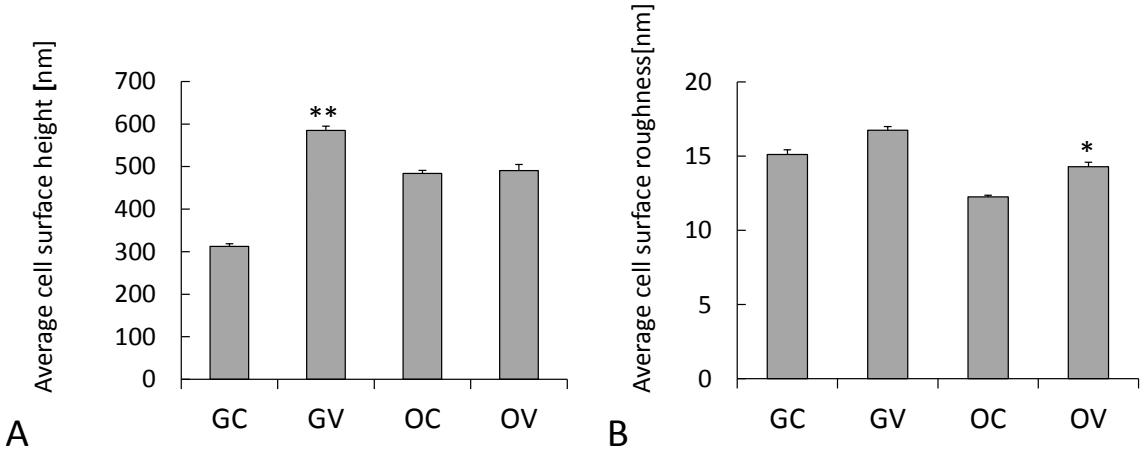

Figure 3.4. Average cell surface height of MSCs. Average cell surface height of GV group is 87% higher than GC (A). Under osteogenic conditions, average cell surface roughness value is 22% higher in vibration group (B). For GC: n=16, GV:n=14, OC: n=25, OV: n=10 sample were analyzed. (*: $p<0.05$, **: $p<0.01$)

Mechanical properties of cells are mainly determined by the cytoskeleton structure which is combination of polymeric networks of actin, microtubules, and intermediate filaments. Actin cytoskeleton is mainly responsible for cell motility and

shape changes during the cell cycle and in response to extracellular stimuli (Cai et al., 2010). AFM is the one of the best microscopy technique that provide detailed information about cytoskeleton structure with its high lateral resolution (Cai et al., 2010) (Berdyyeva et al., 2005) (Rotsch and Radmacher, 2000) AFM analysis showed that LMHF vibrations and osteogenic conditions increased the average cell surface height of MSCs and average nucleus height. Under osteogenic conditions, average cell surface roughness was elevated by mechanical stimulation. Nucleus height was also increased by mechanical stimulation and osteogenic induction. Moreover, fluorescent microscopy studies revealed that mean signal intensity/cell number values indicating the amount of actin content in the cell increased with osteogenic induction and the vibration application. Thickness of the actin fibers got increased with the vibration, whereas osteogenic induction made significantly thinner the actin fibers.

Our results indicate that LMHF mechanical vibrations are anabolic to cytoskeleton of MSCs. It may increase the expression level of cytoskeleton forming proteins or decrease their degradation in protein or mRNA level. This mechanical stimulation also significantly effects to the average nucleus height of MSCs. This incensement maybe related with lamin proteins. Lamin proteins are type V intermediate filaments and play significant role in determination of nuclear size, shape and integrity (Prokocimer et al., 2009). Lamin proteins in particular Lamin A and C are transcriptional regulators and effect MCSs differentiation in a way that decreased lamin A/C expression bias MSCs differentiation away from osteogenesis while enhancing adipogenesis (Akter et al., 2009).The role of cytoskeleton in determination of nuclear shape either directly or via interacting with SUN-/KASH- domain protein complexes that binds lamins was also elucidated (Prokocimer et al., 2009). Increased cytoskeletal content might change lamin A/C expression, and regulate the osteogenesis. This relationship has yet to be identified with further studies.

In AFM studies cells were imaged without fixation (Berdyyeva et al., 2005).We were planning to perform AFM imaging of living cells with “Fluid cell”, unfortunately equipment limitations do not allow us to do that. Surface topography properties is directly related with organization of submembrane and intracellular structures lying under membrane and submembraneous cytoskeleton have been visualized by tapping mode AFM already (Chang et al., 1993) (Grimellec and Cilegiocondi, 1997). Here in this study, we correlated the Average cell surface height and roughness data with changes in cytoskeleton structure.

3.4. Immunostaining and Fluorescent Microscopy

Thickness of actin fibers that cells contain were differed significantly with vibration and osteogenic treatment. Vibrated MSCs in growth medium have 46% thicker fibers ($p=0.04$) compared to control group. In osteogenic conditions again vibration increased the thickness by 14% ($p=0.01$). (figure 3.6 A).

Mean signal intensity per cell ratios were significantly affected by mechanical stimulation. In growth medium, this ratio is increased 20% with mechanical stimulation ($p=0.03$). In osteogenic conditions this increasement is 25% ($p<0.01$) (figure 3.6 B).

Pixel frequency analysis showed that cytoskeleton micrographs of vibrated MSCs contain more pixels with higher signal intensity. Also, pixels with higher intensity are more frequently found in vibrated MSCs compared with non-vibrated MSCs under osteogenic conditions (figure 3.7 A-B).

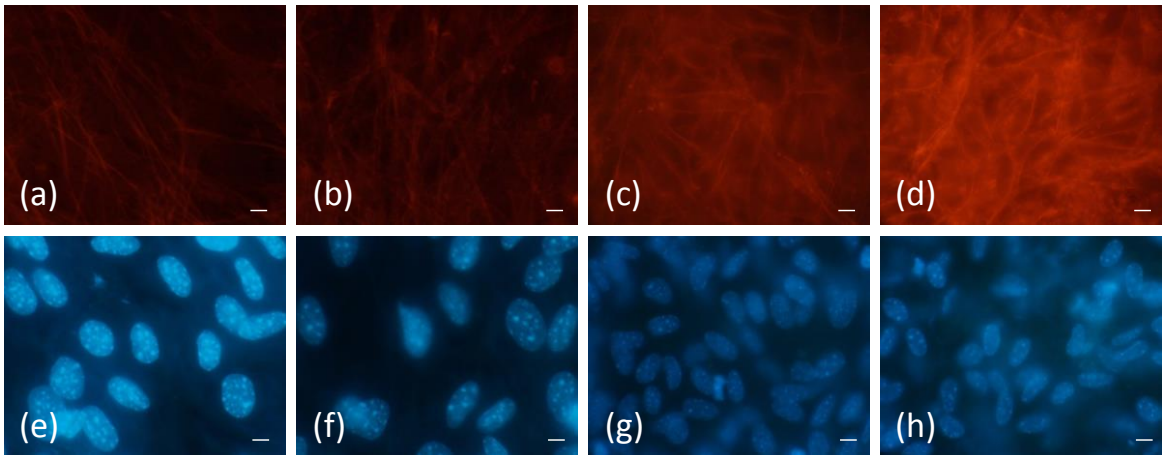

Figure 3.5. Representative fluorescent micrographs for phalloidin (red) and DAPI (blue) stains from (**a, e**) GC cells, (**b, f**) GV cells, (**c, g**) OC cells and (**d, h**) OV cells (Scale Bar: 10µm).

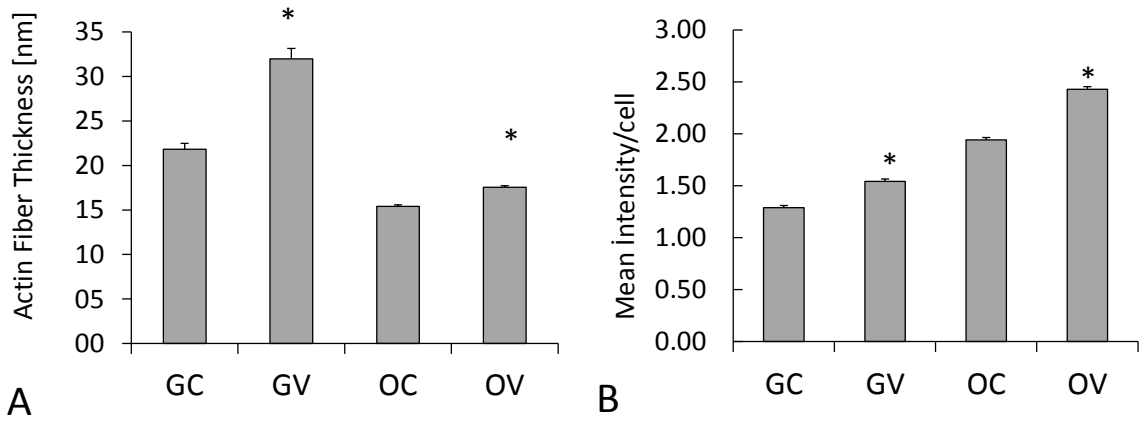

Figure 3.6. Immunostaining and fluorescent microscopy results. In both, growth and osteogenic, conditions, mechanical stimulation increased the actin fiber thickness of cells by 46% and 14%. (A). Under osteogenic conditions mean signal intensity per cell number increased by 25%, under growth conditions it is elevated with mechanical stimulation by 20% (B). 20 images were analyzed for each group. (*: $p<0.05$, **: $p<0.01$)

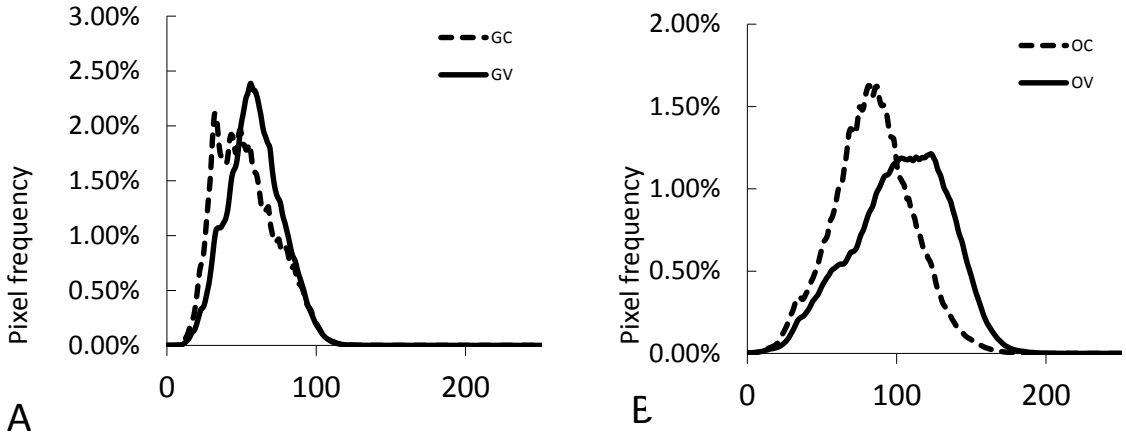

Figure 3.7. Immunostaining and fluorescent microscopy results. Pixel frequency analysis showed that cytoskeleton micrographs of vibrated MSCs contain more pixels with higher signal intensity under both growth (A) and osteogenic (B) conditions. 20 images were analyzed for each group.

Cytoskeleton reorganization is essential for MSCs to express osteogenic markers under osteogenic conditions and in response mechanical stimulations (Chen et al., 2010). It was reported that actin cytoskeleton structure of MSCs differs significantly under osteogenic conditions. Parallel oriented actin fibers acrosing cytoplasm became more cortical organization (Pablo Rodríguez et al., 2004)Also actin fibers of differentiated cells are organized as thinner dense meshwork, whereas MSCs actins are thick bundles (Titushkin and Cho, 2014). Our findings are consistent with previous ones. We found that MSCs under osteogenic conditions have more dense actin structure

at the end of 7 day-induction. We also showed that actin stress fibers had thinner with osteogenic induction. Intact actin cytoskeleton is needed for mechanotrunsduction in MSCs and bone cells (Ajubi et al., 1996) (Chen et al., 2000)). When these cells are subjected to mechanical stimulation, their cytoskeleton structure is also altered. It was reported that in undifferentiated state MSCs has peripheral fibers on the contours of the cell and others crossing the cytoplasm without particular orientation. Hoop stretch exposure made fibers more organized on the long axes and thicker (Zhao et al., 1995). Our data show that, mechanical vibrations have no effect on the fiber orientation, only increase the thickness of the fibers. This orientation effects may be related with the different mechanosensation cascades working with different stimuli.

3.5. Gene Expression Analysis

Gene expression patterns as tested with real time RT-PCR normalized to GC data confirmed the process of osteogenesis with the significant increases in osteogenic markers as Runx2 and OCN (osteocalcin) without any evidence related to effect of vibrations (figure 3.8). From ultrastructural elements, β-actin showed close to two-fold increase ($P = 0.01$) during osteogenesis compared to GC cells, again without any potential effect from mechanical vibrations. Osteogenesis also increased the expression of PTK2 (focal adhesion kinase) more than 20-fold for osteogenic cells ($P < 0.01$) compared to GC cells. Interestingly, GV group also had a similar increase ($P < 0.01$) in the expression of PTK2 compared to GC group, with similar expression levels compared to osteogenic groups. Vibrations significantly ($P < 0.01$) increased Runx2 mRNA levels in stem cells during osteogenesis.

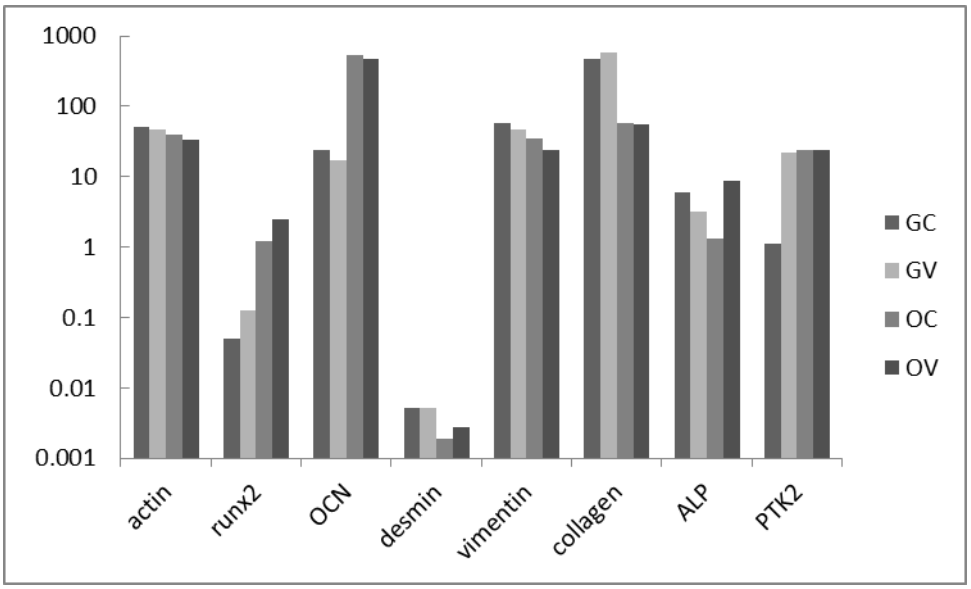

Figure 3.8. Quantitative RT-PCR Results confirmed the osteogenesis of stem cells by significant increase in osteogenic markers runx2 and OCN. No significant elevation of cytoskeletal elements was observed. Expression level of PTK2 increased around 20 fold by both effect mechanical vibration and osteogenic induction separately ($p<0.01$).

Gene expression analysis is more focused on osteogenic markers and cytoskeletal elements. There is no significant change in the expression of osteogenic markers and cytoskeletal elements related with mechanical vibrations. Interesting data in this part is that expression level of focal adhesion kinase (PTK2) is significantly increased with mechanical vibrations. Protein focal adhesion kinase plays role in cellular adhesion, migration and signaling by interacting cell cytoskeleton with extracellular matrix proteins. This result may indicate that cells become more sensitive to mechanical vibrations by increasing connections with its microenvironment.

CHAPTER 4

CONCLUSION

In this study the aim was to identify early effects of mechanical stimulation to ultrastructure of MSCs during early osteogenic commitment. 9-day cell culture study was performed either by using Growth medium or Osteogenic medium and LMHF vibrations applied to experiment groups for 15 min/day. MSCs were imaged with AFM and fluorescent microscopy and then images were analyzed. Also effect of LMHF vibrations on cell growth and expression of particular genes were investigated.

Our results indicate that MSCs alter their ultrastructure in response to applied LMHF mechanical vibrations. Immunostaining and fluorescent microscopy experiments showed that there is significant incresement in main cytoskeleton element actin. Consistent with this, AFM experiments showed that LMHF vibrations increased cellular height and roughness of cells significantly. Furthermore, we showed that MSCs response to altered mechanical forces by increasing expression of PTK2 which connects cells to its microenvironment.

REFERENCES

Ajubi, N.E., Klein-Nulend, J., Nijweide, P.J., Vrijheid-Lammers, T., Alblas, M.J., Burger, E.H., 1996. Pulsating fluid flow increases prostaglandin production by cultured chicken osteocytes--a cytoskeleton-dependent process. Biochem. Biophys. Res. Commun. 225, 62–8.

Alenghat, F.J., Ingber, D.E., 2002. Mechanotransduction: all signals point to cytoskeleton, matrix, and integrins. Sci. STKE 2002, pe6.

Arnsdorf, E.J., Tummala, P., Castillo, A.B., Zhang, F., Jacobs, C.R., 2010. The epigenetic mechanism of mechanically induced osteogenic differentiation. J. Biomech. 43, 2881–6.

Berdyyeva, T., Woodworth, C.D., Sokolov, I., 2005. Visualization of cytoskeletal elements by the atomic force microscope. Ultramicroscopy 102, 189–98.

Bershadsky, A.D., Balaban, N.Q., Geiger, B., 2003. Adhesion-dependent cell mechanosensitivity. Annu. Rev. Cell Dev. Biol. 19, 677–95.

Bonewald, L.F., Johnson, M.L., 2008. Osteocytes, mechanosensing and Wnt signaling. Bone 42, 606–15.

Cai, X., Xing, X., Cai, J., Chen, Q., Wu, S., Huang, F., 2010. Connection between biomechanics and cytoskeleton structure of lymphocyte and Jurkat cells: An AFM study. Micron 41, 257–62.

Caplan, A., 2005. Mesenchymal Stem Cells : Cell-Based Reconstructive Therapy 11, 1198–1211.

Case, N., Rubin, J., 2010. Beta-catenin--a supporting role in the skeleton. J. Cell. Biochem. 110, 545–53.

Chang, L., Kious, T., Yorgancioglu, M., Keller, D., Pfeiffer, J., 1993. Cytoskeleton of living, unstained cells imaged by scanning force microscopy. Biophys. J. 64, 1282–6.

Chen, J.-H., Liu, C., You, L., Simmons, C. a, 2010. Boning up on Wolff's Law: mechanical regulation of the cells that make and maintain bone. J. Biomech. 43, 108–18.

Chen, N.X., Ryder, K.D., Pavalko, F.M., Turner, C.H., Burr, D.B., Qiu, J., Duncan, R.L., 2000. Ca(2+) regulates fluid shear-induced cytoskeletal reorganization and gene expression in osteoblasts. Am. J. Physiol. Cell Physiol. 278, C989–97.

Darling, E.M., Topel, M., Zauscher, S., Vail, T.P., Guilak, F., 2008. Viscoelastic properties of human mesenchymally-derived stem cells and primary osteoblasts, chondrocytes, and adipocytes. J. Biomech. 41, 454–64.

David, V., Martin, A., Lafage-Proust, M.-H., Malaval, L., Peyroche, S., Jones, D.B., Vico, L., Guignandon, A., 2007. Mechanical loading down-regulates peroxisome proliferator-activated receptor gamma in bone marrow stromal cells and favors osteoblastogenesis at the expense of adipogenesis. Endocrinology 148, 2553–62.

Ding, D.-C., Shyu, W.-C., Lin, S.-Z., 2011. Mesenchymal stem cells. Cell Transplant. 20, 5–14.

Discher, D.E., Mooney, D.J., Zandstra, P.W., 2009. Growth factors, matrices, and forces combine and control stem cells. Science 324, 1673–7.

Fritton, S.P., McLeod, K.J., Rubin, C.T., 2000. Quantifying the strain history of bone: spatial uniformity and self-similarity of low-magnitude strains. J. Biomech. 33, 317–25.

Frost, H.M., 1990a. Skeletal structural adaptations to mechanical usage (SATMU): 1. Redefining Wolff's Law: The bone modeling problem. Anat. Rec. 226, 403–413.

Frost, H.M., 1990b. Skeletal structural adaptations to mechanical usage (SATMU): 2. Redefining Wolff's Law: The remodeling problem. Anat. Rec. 226, 414–422.

Garman, R., Rubin, C., Judex, S., 2007. Small oscillatory accelerations, independent of matrix deformations, increase osteoblast activity and enhance bone morphology. PLoS One 2, e653.

Grimellec, C.L.E., Cilegiocondi, M., 1997. Simultaneous imaging of the surface and the submembraneous cytoskeleton in living cells by tapping mode atomic force microscopy 320, 637–643.

Hadjidakis, D.J., Androulakis, I.I., 2006. Bone remodeling. Ann. N. Y. Acad. Sci. 1092, 385–96.

Heinonen, a, Oja, P., Kannus, P., Sievänen, H., Haapasalo, H., Mänttäri, a, Vuori, I., 1995. Bone mineral density in female athletes representing sports with different loading characteristics of the skeleton. Bone 17, 197–203.

Jacobs, C.R., Temiyasathit, S., Castillo, A.B., 2010. Osteocyte Mechanobiology and Pericellular Mechanics. Annu. Rev. Biomed. Eng. 12, 369–400.

Jones, H.H., Priest, J.D., Hayes, W.C., Tichenor, C.C., Nagel, D.A., 2007. Humeral hypertrophy in response to exercise in Response to Exercise 204–208.

Judex, S., Garman, R., Squire, M., Donahue, L.-R., Rubin, C., 2004. Genetically based influences on the site-specific regulation of trabecular and cortical bone morphology. J. Bone Miner. Res. 19, 600–6.

Judex, S., Lei, X., Han, D., Rubin, C., 2007. Low-magnitude mechanical signals that stimulate bone formation in the ovariectomized rat are dependent on the applied frequency but not on the strain magnitude. J. Biomech. 40, 1333–9.

Krause, J.R., 2007. Bone Marrow Overview. In: Hematology Clinical Principles and Applications. Saunders, pp. 193–202.

Krum, S. a, Miranda-Carboni, G. a, Hauschka, P. V, Carroll, J.S., Lane, T.F., Freedman, L.P., Brown, M., 2008. Estrogen protects bone by inducing Fas ligand in osteoblasts to regulate osteoclast survival. EMBO J. 27, 535–45.

Lang, T., LeBlanc, A., Evans, H., Lu, Y., Genant, H., Yu, A., 2004. Cortical and trabecular bone mineral loss from the spine and hip in long-duration spaceflight. J. Bone Miner. Res. 19, 1006–12.

Lau, E., Al-Dujaili, S., Guenther, A., Liu, D., Wang, L., You, L., 2010. Effect of low-magnitude, high-frequency vibration on osteocytes in the regulation of osteoclasts. Bone 46, 1508–15.

Liu, J., Wang, H., Zuo, Y., Farmer, S.R., 2006. Functional interaction between peroxisome proliferator-activated receptor gamma and beta-catenin. Mol. Cell. Biol. 26, 5827–37.

Luu, Y.K., Capilla, E., Rosen, C.J., Gilsanz, V., Pessin, J.E., Judex, S., Rubin, C.T., 2009. Mechanical Stimulation of Mesenchymal Stem Cell Proliferation and Differentiation Promotes Osteogenesis While Preventing Dietary-Induced Obesity 24, 50–61.

Luu, Y.K., Pessin, J.E., Judex, S., Rubin, J., Rubin, C.T., 2009. Mechanical Signals As a Non-Invasive Means to Influence Mesenchymal Stem Cell Fate, Promoting Bone and Suppressing the Fat Phenotype. Bonekey Osteovision 6, 132–149.

Meloni, M.A., Galleri, G., Pani, G., Saba, A., Pippia, P., Cogoli-Greuter, M., 2011. Space flight affects motility and cytoskeletal structures in human monocyte cell line J-111. Cytoskeleton (Hoboken). 68, 125–37.

Norvell, S.M., Alvarez, M., Bidwell, J.P., Pavalko, F.M., 2004. Fluid shear stress induces beta-catenin signaling in osteoblasts. Calcif. Tissue Int. 75, 396–404.

Ozcivici, E., Garman, R., Judex, S., 2007. High-frequency oscillatory motions enhance the simulated mechanical properties of non-weight bearing trabecular bone. J. Biomech. 40, 3404–11.

Ozcivici, E., Luu, Y.K., Rubin, C.T., Judex, S., 2010. Low-level vibrations retain bone marrow's osteogenic potential and augment recovery of trabecular bone during reambulation. PLoS One 5, e11178.

Pablo Rodríguez, J., González, M., Ríos, S., Cambiazo, V., 2004. Cytoskeletal organization of human mesenchymal stem cells (MSC) changes during their osteogenic differentiation. J. Cell. Biochem. 93, 721–731.

Peacock, M., Koller, D.., Fishburn, T., 2005. Sex-Specific and Non-Sex-Specific Quantitative Trait Loci Contribute to Normal Variation in Bone Mineral Density in Men. J. Clin. Endocrinol. Metab. 90, 3060–3066.

Prokocimer, M., Davidovich, M., Nissim-Rafinia, M., Wiesel-Motiuk, N., Bar, D.Z., Barkan, R., Meshorer, E., Gruenbaum, Y., 2009. Nuclear lamins: key regulators of nuclear structure and activities. J. Cell. Mol. Med. 13, 1059–85.

Robling, A.G., Castillo, A.B., Turner, C.H., 2006. Biomechanical and molecular regulation of bone remodeling. Annu. Rev. Biomed. Eng. 8, 455–98.

Rodan, G.A., 2003. The development and function of the skeleton and bone metastases. Cancer 97, 726–732.

Rosen, Evan D, MacDougald, O.A., 2006. Adipocyte differentiation from the inside out. Nat Rev Mol Cell Biol 7, 885–896.

Rosenberg, N., 2003. The role of the cytoskeleton in mechanotransduction in human osteoblastlike cells. Hum. Exp. Toxicol. 22, 271–274.

Rotsch, C., Radmacher, M., 2000. Drug-induced changes of cytoskeletal structure and mechanics in fibroblasts: an atomic force microscopy study. Biophys. J. 78, 520–35.

Roy V. Talmage, and J.R.E., 1958. REMOVAL OF CALCIUM FROM BONE AS INFLUENCED BY THE PARATHYROIDS. Endocrinology 62, 717–722.

Rubin, C., Judex, S., Qin, Y.-X., 2006. Low-level mechanical signals and their potential as a non-pharmacological intervention for osteoporosis. Age Ageing 35 Suppl 2, ii32–ii36.

Rubin, C., Recker, R., Cullen, D., Ryaby, J., McCabe, J., McLeod, K., 2004. Prevention of postmenopausal bone loss by a low-magnitude, high-frequency mechanical stimuli: a clinical trial assessing compliance, efficacy, and safety. J. Bone Miner. Res. 19, 343–51.

Rubin, C., Xu, G., Judex, S., 2001. The anabolic activity of bone tissue, suppressed by disuse, is normalized by brief exposure to extremely low-magnitude mechanical stimuli. FASEB J. 15, 2225–9.

Ruimerman, R., 2005. Modeling and remodeling in bone tissue. Technische Universiteit Eindhoven.

Salo, J., Metsikkö, K., Palokangas, H., Lehenkari, P., Väänänen, H.K., 1996. Bone-resorbing osteoclasts reveal a dynamic division of basal plasma membrane into two different domains. J. Cell Sci. 109 (Pt 2, 301–7.

Santos, A., Bakker, A.D., Zandieh-Doulabi, B., de Blieck-Hogervorst, J.M. a, Klein-Nulend, J., 2010. Early activation of the beta-catenin pathway in osteocytes is mediated by nitric oxide, phosphatidyl inositol-3 kinase/Akt, and focal adhesion kinase. Biochem. Biophys. Res. Commun. 391, 364–9.

Sehmisch, S., Galal, R., Kolios, L., Tezval, M., Dullin, C., Zimmer, S., Stuermer, K.M., Stuermer, E.K., 2009. Effects of low-magnitude, high-frequency mechanical stimulation in the rat osteopenia model. Osteoporos. Int. 20, 1999–2008.

Short, B., Brouard, N., Occhiodoro-scott, T., Ramakrishnan, A., Simmons, P.J., 2004. Mesenchymal Stem Cells 34, 565–571.

Sommerfeldt, D., Rubin, C., 2001. Biology of bone and how it orchestrates the form and function of the skeleton. Eur. Spine J. 10, S86–S95.

Tai, B.C.U., Du, C., Gao, S., Wan, A.C. a, Ying, J.Y., 2010. The use of a polyelectrolyte fibrous scaffold to deliver differentiated hMSCs to the liver. Biomaterials 31, 48–57.

Titushkin, I., Cho, M., 2014. Distinct Membrane Mechanical Properties of Human Mesenchymal Stem Cells Determined Using Laser Optical Tweezers. Biophys. J. 90, 2582–2591.

Uzer, G., Manske, S.L., Chan, M.E., Chiang, F.-P., Rubin, C.T., Frame, M.D., Judex, S., 2012. Separating Fluid Shear Stress from Acceleration during Vibrations in Vitro: Identification of Mechanical Signals Modulating the Cellular Response. Cell. Mol. Bioeng. 5, 266–276.

Uzer, G., Pongkitwitoon, S., Ete Chan, M., Judex, S., 2013. Vibration induced osteogenic commitment of mesenchymal stem cells is enhanced by cytoskeletal remodeling but not fluid shear. J. Biomech. 46, 2296–302.

Väänänen, H.K., Zhao, H., Mulari, M., Halleen, J.M., 2000. The cell biology of osteoclast function. J. Cell Sci. 113 (Pt 3, 377–81.

Verschueren, S.M.P., Roelants, M., Delecluse, C., Swinnen, S., Vanderschueren, D., Boonen, S., 2004. Effect of 6-month whole body vibration training on hip density, muscle strength, and postural control in postmenopausal women: a randomized controlled pilot study. J. Bone Miner. Res. 19, 352–9.

You, J., 2000. Substrate Deformation Levels Associated With Routine Physical Activity Are Less Stimulatory to Bone Cells Relative to Loading-Induced Oscillatory Fluid Flow. J Biomech Eng. 122, 387–393.

Yourek, G., Hussain, M. a, Mao, J.J., 2007. Cytoskeletal changes of mesenchymal stem cells during differentiation. ASAIO J. 53, 219–28.

Zaidi, M., Moonga, B.S., Abe, E., 2002. Calcitonin and bone formation: a knockout full of surprises. J. Clin. Invest. 110, 1769–1771.

Zaman, G., Jessop, H.L., Muzylak, M., De Souza, R.L., Pitsillides, A.A., Price, J.S., Lanyon, L.L., 2006. Osteocytes Use Estrogen Receptor α to Respond to Strain but Their ERα Content Is Regulated by Estrogen. J. Bone Miner. Res. 21, 1297–1306.

Zhao, S., Suciu, A., Ziegler, T., Moore, J.E., Bürki, E., Meister, J.-J., Brunner, H.R., 1995. Synergistic Effects of Fluid Shear Stress and Cyclic Circumferential Stretch on Vascular Endothelial Cell Morphology and Cytoskeleton. Arterioscler. Thromb. Vasc. Biol. 15 , 1781–1786.

APPENDIX A

AFM IMAGE PROCESSING

Before performing the analyses, AFM images were processed. Firstly, all data on an image were leveled by fitted plane through three points (figure A.1). The three point leveling tool can be used for leveling very complicated structures. The user can simply mark three points in the image that should be at the same level, and then click apply. The plane is computed from these three points and is subtracted from the data. Following that, data were fitted by polynomial of second order and then background were subtracted by remove polynomial background tool (figure A.2). After horizontal scars were corrected if there were any, minimum value on the data was shifted to zero (figure A.3) in order to get comparable measurements from each image.

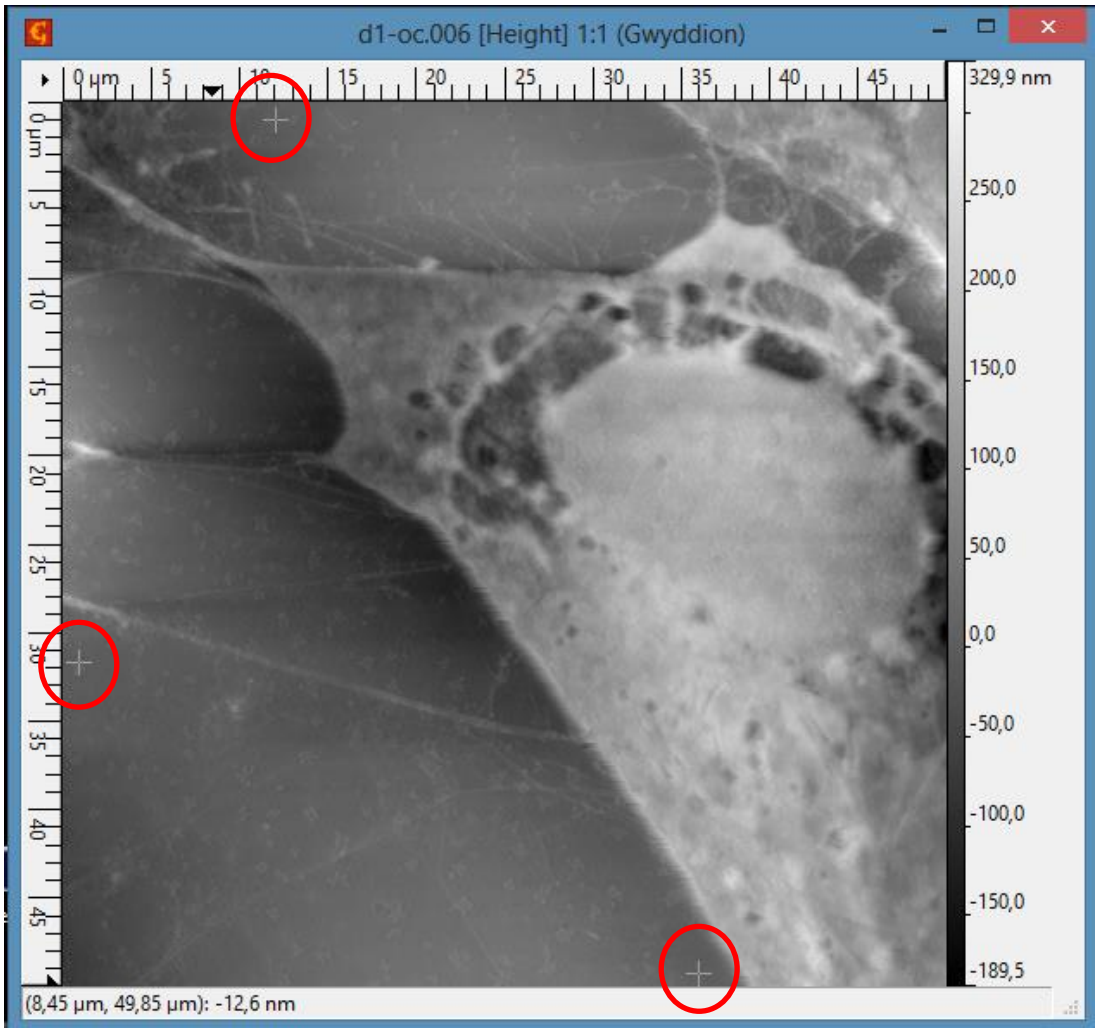

Figure A.1. Three point leveling tool. Levels data by plane obtained by clicking on three points within data window. The three values can be averaged over a small area around the selected point. The Three Point Leveling tool can be used for leveling complicated surface structures. The user can simply mark three points in the image that should be at the same level, and then click Apply. The plane is computed from these three points and is subtracted from the data.

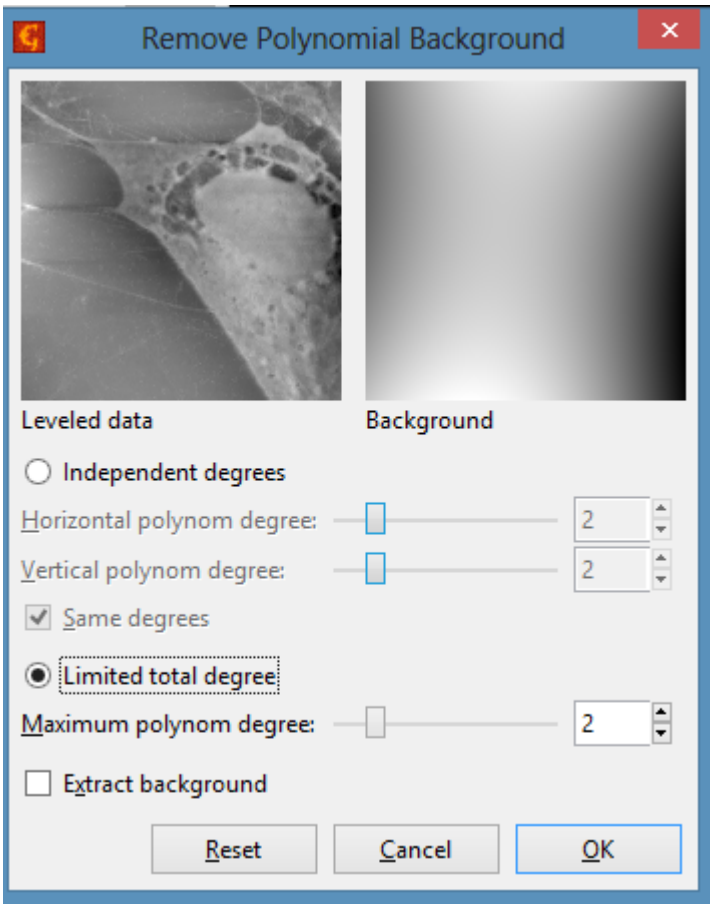

Figure A.2. Remove polynomial background. Levels rows or columns by fitting and subtracting polynomials. Fits data by a polynomial of the given order and subtracts this polynomial. Maximum polynomial degree is adjusted to 2 inorder to prevent data loss with higher degrees.

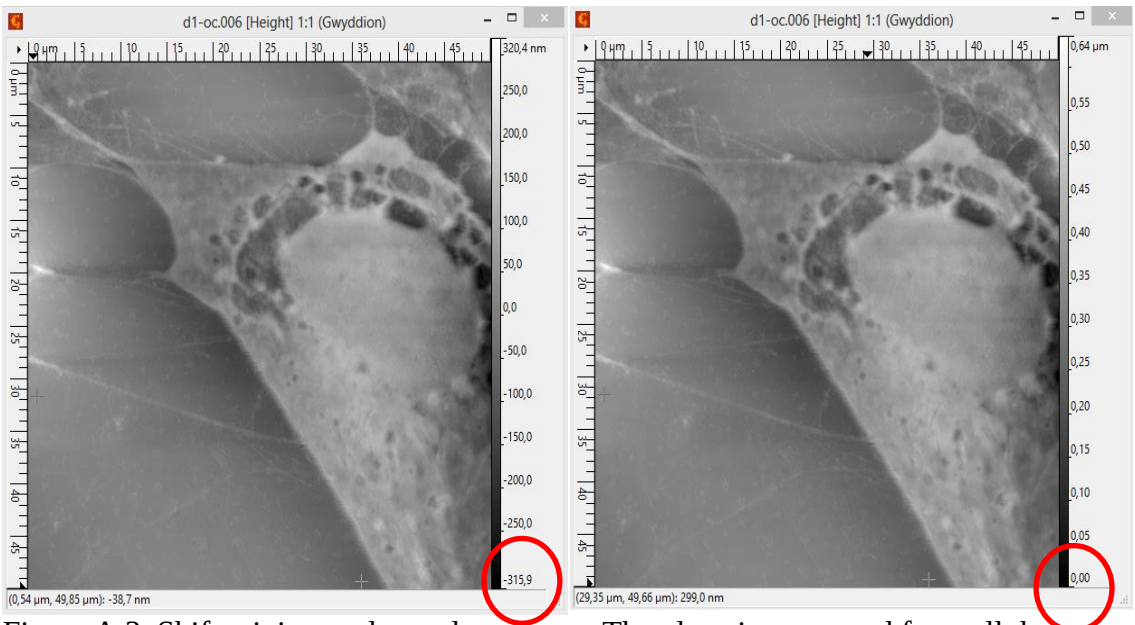

Figure A.3. Shift minimum data value to zero. The plane is computed from all the image points and is subtracted from the data.

Average Cell Surface Height Analysis

By using extract profile tool five section from cytoplasmic regions of cells were taken and y values of these sections were evaluated as cell surface height of cells (figure A.4).

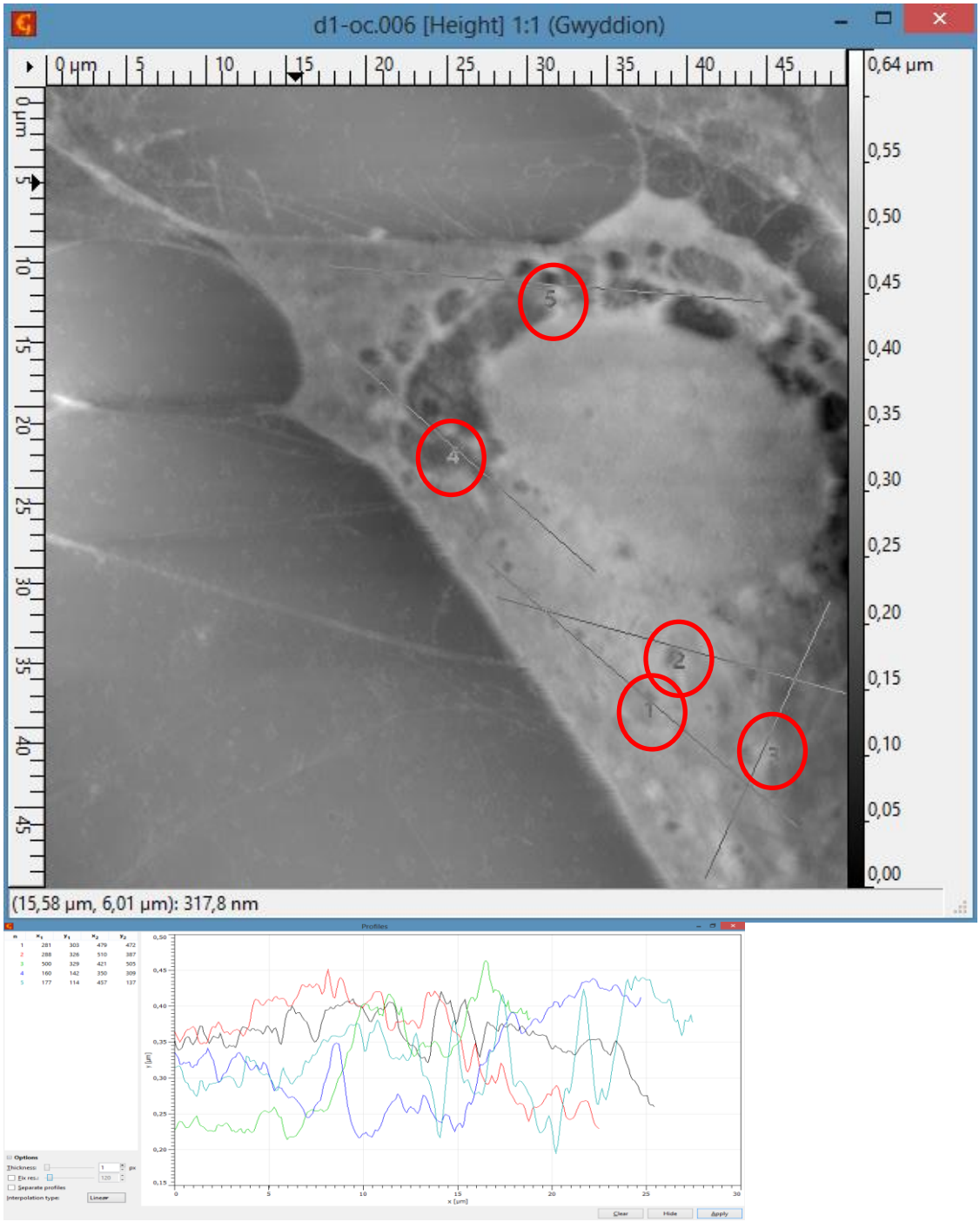

Figure A.4. Extract profile tool. Extracts profiles of the data field and puts them to separate graphs. These graphs can be further processed Five sections from cytoplasmic region of cell surface were taken and then cell surface height were calculated on excel by using y values of profiles.

Average Cell Surface Roughness

Calculate roughness parameters tool was used for this analysis. Roughness average (Ra) is arithmetical mean deviation meaning that the average deviation of all points of roughness profile from a mean line over the evaluation length. Average of five different Ra values was evaluated as average cell surface roughness for each cell (figure A.5).

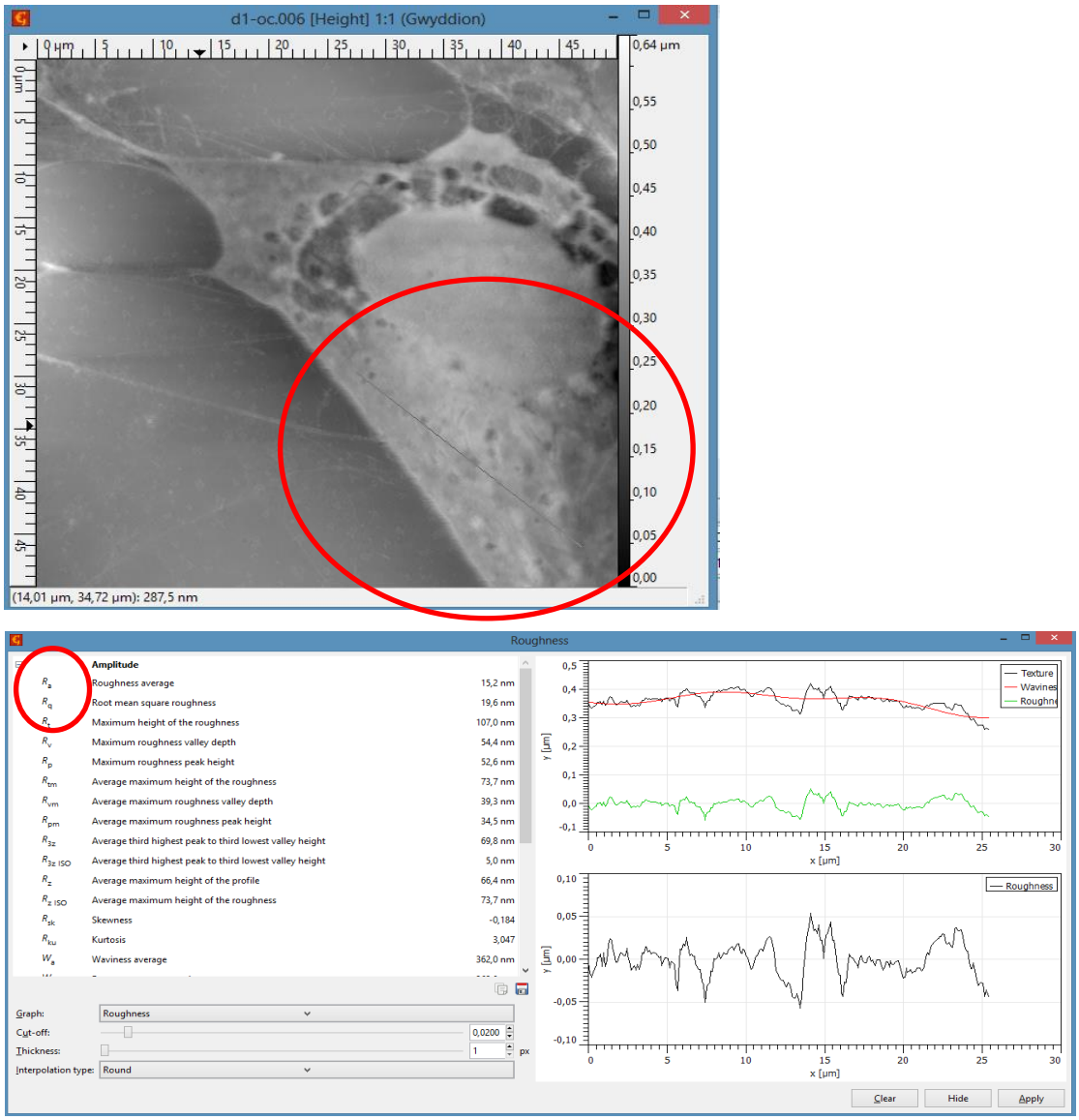

Figure A.5. Calculate roughness parameters tool. Evaluates standardized one-dimensional roughness parameters. Ra is roughness average of taken profile.

Average Nucleus Area and Height Analysis

Nucleuses of cells in each image were masked first and then average value and surface area under the masked region were calculated with statistical quantities tool (figure A.6).

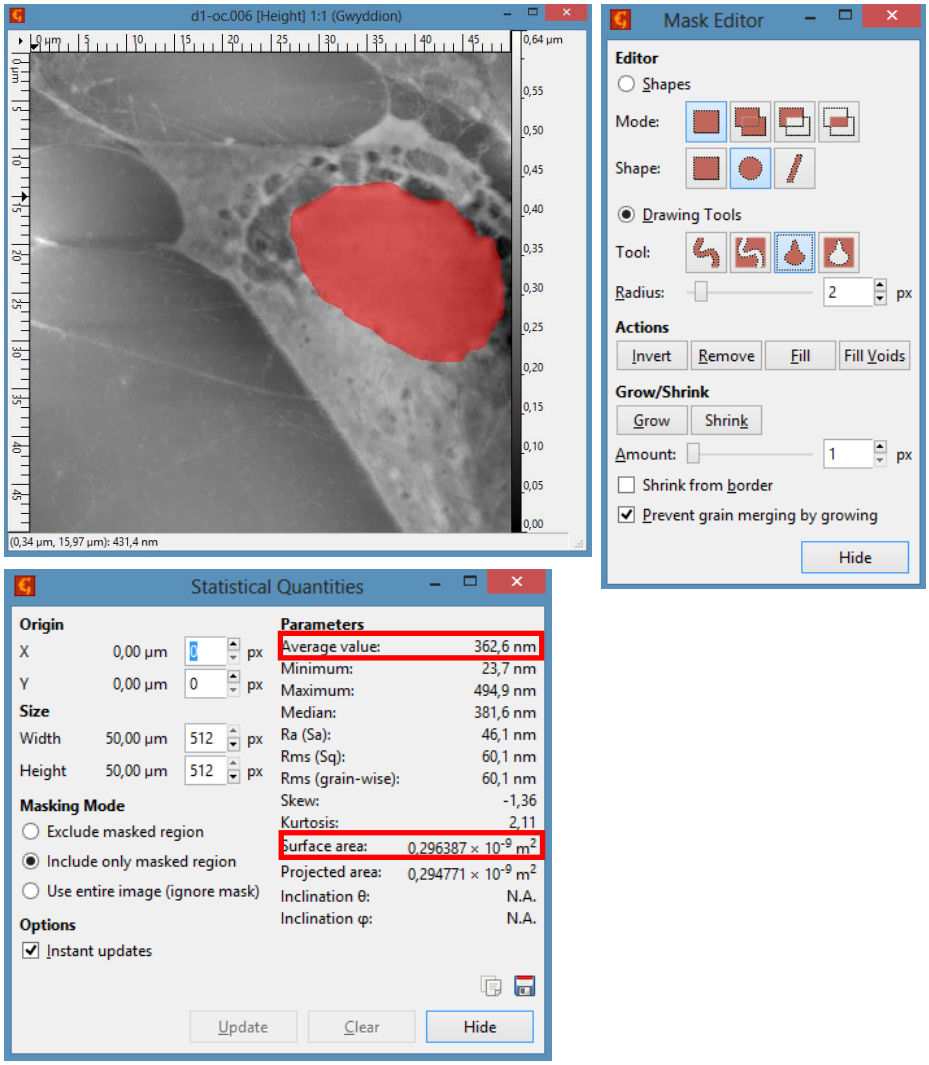

Figure A.6. Nucleus masking. Nucleus of cells was masked with mask editor tool. By using statistical quantities tool, average value of nucleus height and surface area was calculated.

Sample AFM Images

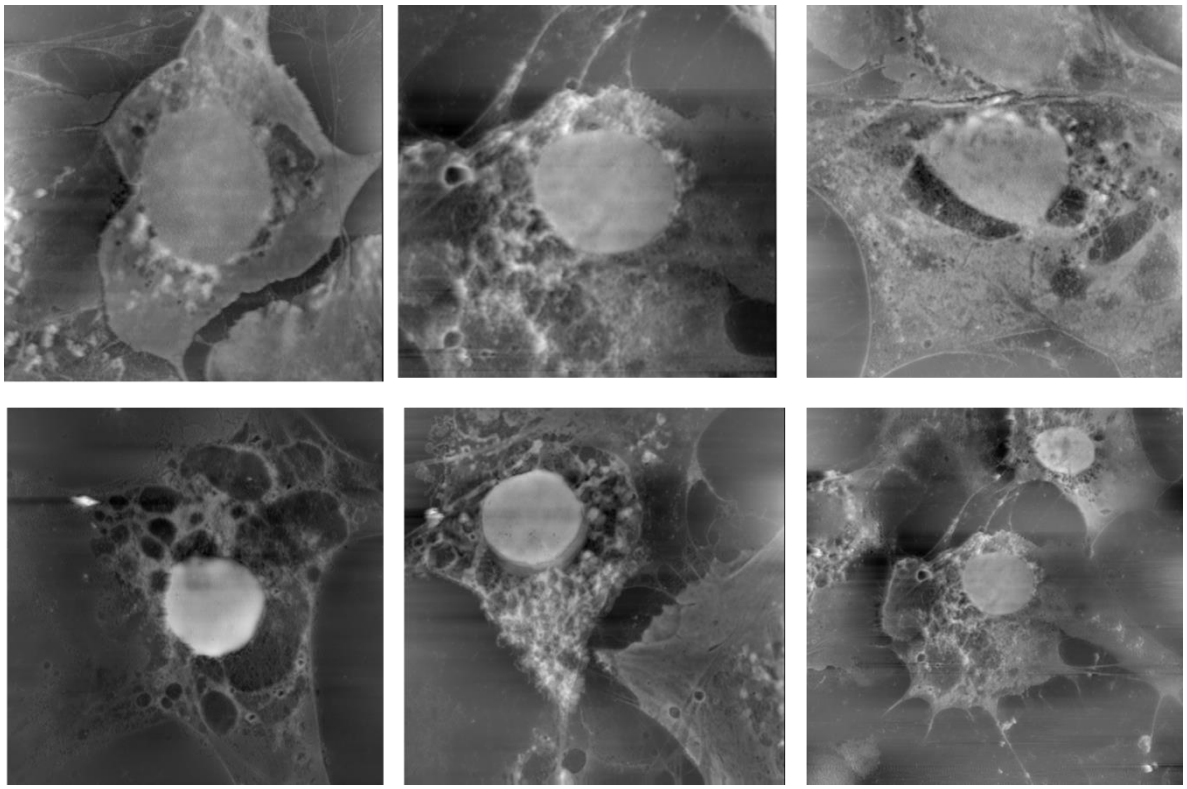

Figure A.7. Examples of 2d AFM images that acquired with Digital Instruments-MMSPM Nanoscope IV.